Effect of nonstoichiometry on the structure and microwave dielectric properties of Ba(Co$_{1/3}$Nb$_{2/3}$)O$_3$ ceramics

F. Azough, C. Leach, R. Freer[*]

Materials Science Centre, School of Materials, University of Manchester, Manchester M1 7HS, UK

Available online 13 March 2006

Abstract

The effect of B-site cation deficiency on the structure and microwave dielectric properties of Ba(Co$_{1/3}$Nb$_{2/3}$)O$_3$ (BCN) was investigated. Stoichiometric and co-deficient compositions based on Ba(Co$_{1/3-x}$Nb$_{2/3}$)O$_3$ [$x = 0.0, 0.01, 0.02, 0.03$ and 0.04] were prepared using the conventional mixed oxide route. Small amounts of V$_2$O$_5$ (0.1 wt%) were added to promote densification. The dielectric loss is very sensitive to the composition; it was found that co-deficiency degraded the microwave dielectric properties. The stoichiometric formulation ($x = 0$) exhibited the best microwave properties. The improvements in the microwave dielectric properties were achieved by increasing the degree of 1:2 cation ordering. The highly ordered, stoichiometric BCN ceramics showed a relative permittivity (ε_r) of 32, quality factor ($Q \times f$) of 66,500 GHz and a negative temperature coefficient of resonant frequency (τ_f) of -10 ppm/°C at 4 GHz.
© 2006 Elsevier Ltd. All rights reserved.

Keyword: Ba(Co$_{1/3}$Nb$_{2/3}$)O$_3$; Dielectric properties; Perovskites

1. Introduction

Complex perovskite oxides based on Ba(B$'_{1/3}$B$''_{2/3}$)O$_3$ (B$'$ = Zn, Co, Ni and Mg; B$''$ = Ta and Nb) are suitable materials for dielectric resonator (DR) applications due to their high dielectric constant, high quality factor, and temperature stability of the resonant frequency.[1–4] Recently, due to the high cost of Ta$_2$O$_5$, niobium based complex perovskites have attracted considerable attention. For example, BCN has a relative permittivity of 32, a quality factor ($Q \times f$) greater than 50,000 GHz and negative temperature coefficient of resonant frequency (τ_f) which can adjusted to zero by Zn substitution.[5–8] BCN crystallizes in either a disordered cubic structure or in an ordered hexagonal structure. The ordered structure results from the 1:2 ordering of B$'$ and B$''$ cations along the $\langle 1\,1\,1 \rangle$ directions of the cubic unit cell. It is well established that B-site cation ordering in complex perovskites has a significant influence on the dielectric losses at microwave frequencies.[9,10] Stoichiometry of the B-site may also affect the rate of 1:2 ordering. Twenty years ago, Desu and O'Bryan[11] made the first attempt to correlate the excellent microwave quality factor of Ba(Zn$_{1/3}$Ta$_{2/3}$)O$_3$ (BZT) with B-site cation stoichiometry. They explained the low-loss behaviour on

the basis of zinc evaporation. They suggested that the loss of zinc from the sample leads to crystallographic distortion, which in turn may promote 1:2 ordering. Kawashima[12] subsequently found that ZnO evaporation caused inhomogeneous densification. The latter problem can be minimised and compensated by muffling the samples in ZnO; however muffling reduced the quality factor.[12] Kim et al.[13] studied the effect of 1:2 ordering in Ba(Zn$_{1/3}$Ta$_{2/3}$)O$_3$ ceramics doped with 0–4 mol% BaWO$_4$ under varying sintering conditions. The sintering atmosphere was either air or ZnO powder muffling. The $Q \times f$ values were extremely low for samples prepared under ZnO-muffling regardless of the degree of 1:2 order. The maximum $Q \times f$ values were 160,000–200,000 GHz at 0.5–1.5 mol% BaWO$_4$ doping. The air sintered samples showed Ba$_7$Ta$_6$O$_{22}$ as the major extra phase. In ZnO-muffled specimens BaWO$_4$ was the dominant extra phase.

In the related materials, Ba(Mg$_{1/3}$Nb$_{2/3}$)O$_3$, Paik et al.[14] found that Mg deficiency had a significant effect on the microwave dielectric properties. They reported an improvement in both density and the dielectric Q value when $x = 0.02$ in Ba(Mg$_{1/3-x}$Nb$_{2/3}$)O$_3$. The densification was explained in terms of enhanced grain boundary mass transport because of the formation of additional lattice defects. Lu and Tsai[15] examined the effect of Ba-deficiency in the analogous Ba(Mg$_{1/3}$Ta$_{2/3}$)O$_3$ (BMT) ceramics and found an improvement in the degree of 1:2 order, sinterability and microwave dielectric properties. Lee et al.[16] also demonstrated that grain growth is significantly faster

in Mg-deficient BMT than in stoichiometric BMT ceramics. In contrast, they found that the nonstoichiometric samples exhibited lower Q values.[16]

Recently, Hughes et al.[17] investigated the system $Ba(Zn_{1/3}Nb_{2/3})O_3$–$Ba(Ga_{1/2}Ta_{1/2})O_3$. For even moderate sintering times, the Zn-deficient phases $Ba_8Zn_1Nb_6O_{24}$ and $Ba_5Nb_4O_{15}$ were formed on the surface of ceramics; the amount of the secondary phase increased with sintering time. Similarly for $Ba[(Zn,Co)_{1/3}Nb_{2/3}]O_3$ ceramics, Azough et al.[18] confirmed the formation of $Ba_8(Co,Zn)_1Nb_6O_{24}$ and $Ba_5Nb_4O_{15}$ as secondary surface phases, as a result of the loss of both zinc and cobalt during sintering.

In the present study, the effect of Co deficiency on the microstructure, structural ordering and microwave dielectric properties of $BaCo_{1/3}Nb_{2/3}O_3$ (BCN) has been investigated.

2. Experimental

Specimens were prepared by a conventional mixed oxide route. High purity (>99.9%) $BaCO_3$, CoO, Nb_2O_5 and V_2O_5 were used as raw materials. The powders were weighed to yield compositions $Ba(Co_{1/3-x}Nb_{2/3})O_3$ (where $x = 0.0$, 0.01, 0.02, 0.03 and 0.04; denoted as X0, X1, X2, X3 and X4, respectively). They were mixed in propan-2-ol with zirconia media for 18 h and calcined at 1100 °C for 4 h. After adding 0.1 wt% V_2O_5 as sintering aid, the powders were again wet milled for 18 h and dried. Pellets were formed by pressing at 100 MPa in cylindrical dies (20 mm diameter). They were then sintered in air at 1450 °C for times of 4, 8 or 12 h in and cooled at 60 °C/h. Selected samples were cooled at rates of 360 or 5 °C/h after sintering. The final dimensions of the sintered products were typically 15.5 mm diameter and 9 mm thick. Densities were determined by the Archimedes method.

Phase identification and crystal structure analysis of sintered products were undertaken using a Philips Analytical X'PERT-MPD X-ray diffraction system employing Cu Kα1 radiation (operating conditions 50 kV and 40 mA). The samples were scanned over the 2θ range 10–70° with a step size of 0.04°; the scan rate was 0.01° 2θ/s.

Microstructures of the sintered ceramics were examined by scanning electron microscopy (SEM) (Philips XL30). Sample surfaces were ground (to 1200 grade SiC) then polished (to 1 μm diamond paste) and coated with carbon prior to SEM analysis. For more detailed microstructural studies, TEM specimens were prepared from the sintered ceramics. After lapping and polishing, discs of 3 mm diameter discs were prepared. These were reduced to a thickness of 30 μm in the centre by mechanical dimpling and then thinned to electron transparency with a Gatan Precision Ion Polishing System (PIPS). The specimens were investigated using a Tecnai G2 TEM operating at 300 kV.

Microwave dielectric properties (ε_r and Q) were determined at ~4 GHz by the parallel plate method.[19] The temperature coefficient of resonant frequency was determined using a silver-plated, aluminium cavity at temperatures between −10 and +60 °C.

3. Results and discussion

The density of undoped stoichiometric BCN (X0) ceramics after sintering at 1450 °C was only 70% theoretical. Samples prepared with Co deficiency exhibited a slight improvement in the sintered density but only achieved 80% of the theoretical values for the formulation with $x = 0.04$ (X4), i.e. $Ba(Co_{0.29}Nb_{0.67})O_3$. Adding 0.1 wt V_2O_5 to the starting powders increased the sintered density to above the 95% theoretical for all formulations. Increasing the sintering time from 4 to 12 h did not have any significant effect on the specimen densities.

X-ray diffraction analysis of the low density, stoichiometric, end member (X0) specimens confirmed a simple cubic structure. In the higher density, non-stoichiometric specimens prepared with sintering aid, the X-ray spectra are characteristic of a 1:2 type, ordered hexagonal structure. Fig. 1 shows an X-ray diffraction spectrum for specimen X3, which is typical for all the non-stoichiometric products. In addition to the primary phase, there is clear evidence of additional phases. The minor peaks, such as those at 27.3° and 30.0° 2θ (Fig. 1 inset), increased in intensity as sample nonstoichiometry (x) increased and also as cooling rate after sintering decreased. These minor peaks occur at very similar 2θ values as those for $Ba_8Zn_1Nb_6O_{24}$ and $Ba_5Nb_4O_{15}$ in $Ba(Zn_{1/3}Nb_{2/3})O_3$ ceramics,[6,18] and are, by analogy, inferred to be $Ba_8Co_1Nb_6O_{24}$ and $Ba_5Nb_4O_{15}$ in this case. The enlarged version of the spectrum (inset, Fig. 1) revealed the presence of superlattice reflections, for example at 17.6° 2θ. Superlattice reflections, indicating 1:2 ordering, were present in the spectra for all high-density specimens; peak intensity increased as the cooling rate after sintering decreased, indicating the enhancement of ordering.

SEM microstructural analysis of the as-fired surfaces of stoichiometric X0 samples revealed only one phase, with a typical grain size of 1 μm after sintering for 4 h. Increasing the sintering time to 12 h led to an increase in grain growth to 3 μm (Fig. 2a). The lack of secondary phases in the X0 samples is in contrast to the behaviour of $Ba(Zn_{1/3}Nb_{2/3})O_3$ (BZN) and $Ba[(Zn,Co_{1/3})Nb_{2/3}]O_3$ (BCZN) ceramics where two types of secondary phases (i.e. $Ba_8Zn_1Nb_6O_{24}$ and $Ba_5Nb_4O_{15}$) are

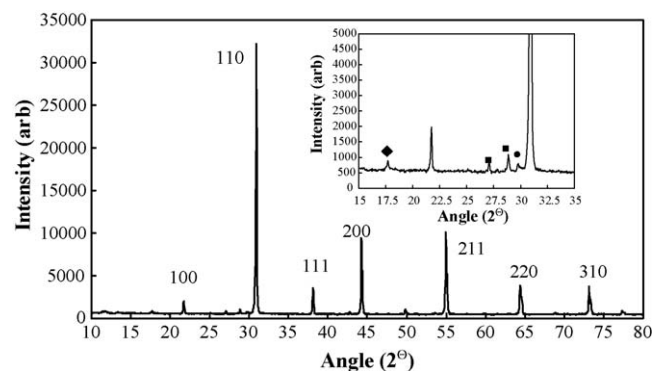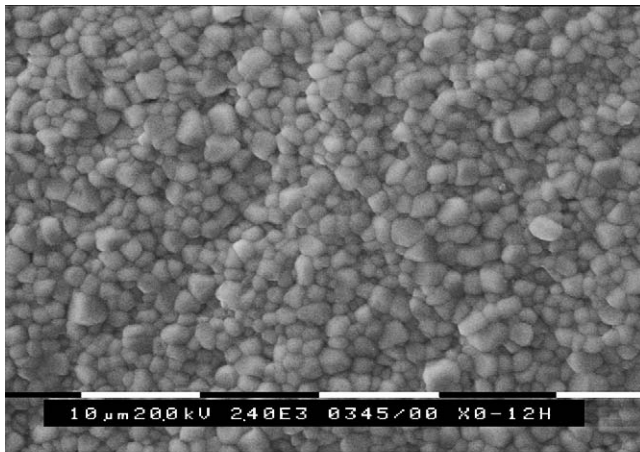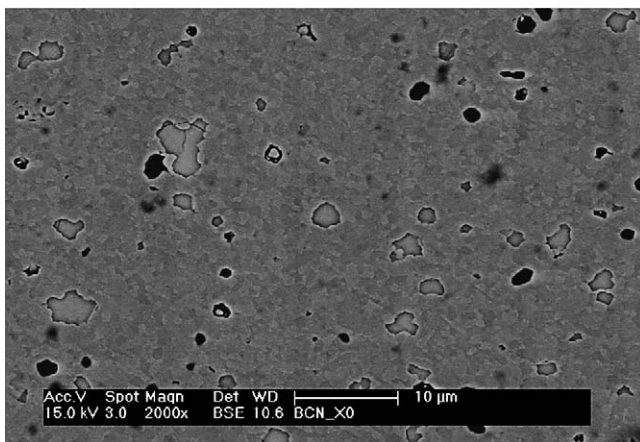Fig. 1. X-ray diffraction spectrum for specimen X3 cooled at 60 °C/h after sintering. The inset is an enlargement of the region between 15° and 25° 2θ. Secondary phases are inferred to be $Ba_8Zn_1Nb_6O_{24}$ (●) and $Ba_5Nb_4O_{15}$ (■); see text. Superlattice peaks for 1:2 ordering are denoted by (♦).
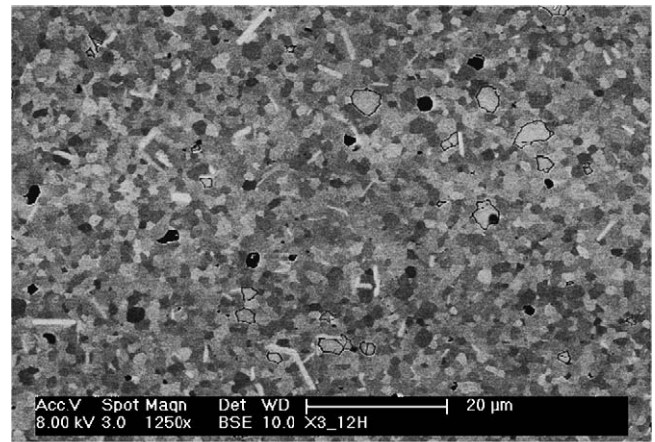
(a)

(b)

Fig. 2. FEGSEM micrographs of sample X0 sintered for 12 h: (a) as-fired surface; no evidence of any secondary phases; (b) backscattered image of polished cross section of the sample indicating the presence of Ba–V–Nb rich secondary phases.
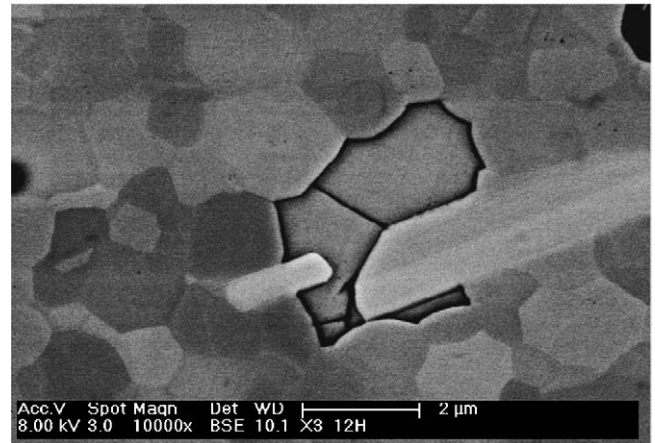

(a)

(b)

Fig. 3. FEGSEM micrographs of sample X3 sintered for 12 h showing the irregularly shaped Ba–V–Nb rich secondary phase and needle shaped grains of $Ba_8Co_1Nb_6O_{24}$.

reported to form on the sample surfaces[17,18] as a result of Zn loss during sintering.

Fig. 2b is a backscattered FEGSEM image of a polished cross section of sample X0. An irregularly shaped second phase, typically 2–3 μm in size, can be seen throughout the microstructure. Energy dispersive analysis (EDS) showed that this phase is rich in (Ba–V–Nb) and possibly acts as liquid phase during sintering process. The irregular shape and absence of any additional X-ray reflections tends to suggest that it is a residual glass product. A low meting point eutectic, as low as 650 °C, has been reported for the system $BaO–V_2O_5–Nb_2O_5$.[20] The effectiveness of V_2O_5 in lowering the sintering temperature of $Ba(Mg_{1/3}Ta_{2/3})O_3$ (BMT) was reported by Huang et al.[21] The addition of as little as 0.25 wt% V_2O_5 lowered the sintering temperature of BMT ceramics by 150 °C. However, there was a direct impact on the dielectric properties and the $Q \times f$ was only 149,000 at 10 GHz.

The as-fired surfaces of co-deficient samples (X1–X4) exhibited no obvious secondary phases, behaving the same as the stoichiometric sample (X0). Backscattered FEGSEM images of the polished surface of sample X3 (Fig. 3a and b) confirm the

presence of the irregularly shaped (Ba–V–Nb) rich phase plus needle shaped grains. EDS analysis of the latter phase indicated that it is rich in Ba–Nb–Co, with a chemical formula close to $Ba_8Co_1Nb_6O_{24}$. Thus the cobalt analogue of BZN may suffer some loss of divalent species during sintering, leading to the formation of an "8-1-6-24" phase. However, evaporation during sintering appears to be much less effective in the cobalt analogue than in BZN, because there no evidence of co-deficient phases on the surface of the specimens and a smaller quantity of secondary phases within the bulk of the material. More detailed microstructural studies by TEM confirmed the composition of the $Ba_8Co_1Nb_6O_{24}$ phase in X3 samples (Fig. 4a). In addition, very small quantities of the cobalt-free phase $Ba_5Nb_4O_{15}$ were identified (Fig. 4b). This reflects the differing behaviour of BZN and BCN; significant amounts of $Ba_8Co_1Nb_6O_{24}$ and $Ba_5Nb_4O_{15}$ were found within the bulk and on the surface of BZN-based ceramics.[2,6,11,17]

There was no evidence of the second phases $Ba_8Co_1Nb_6O_{24}$ and $Ba_5Nb_4O_{15}$ in the microstructure of either X0 or X1 samples. In contrast they were both found in samples X2–X4. Thus deliberately reducing the amount of cobalt in the starting mixture to promote non-stoichiometry is sufficient to form the co-deficient phases when $x \geq 0.02$ in $Ba(Co_{1/3-x}Nb_{2/3})O_3$.
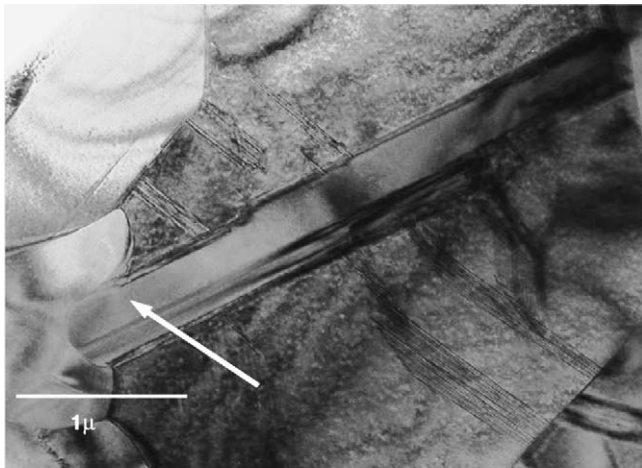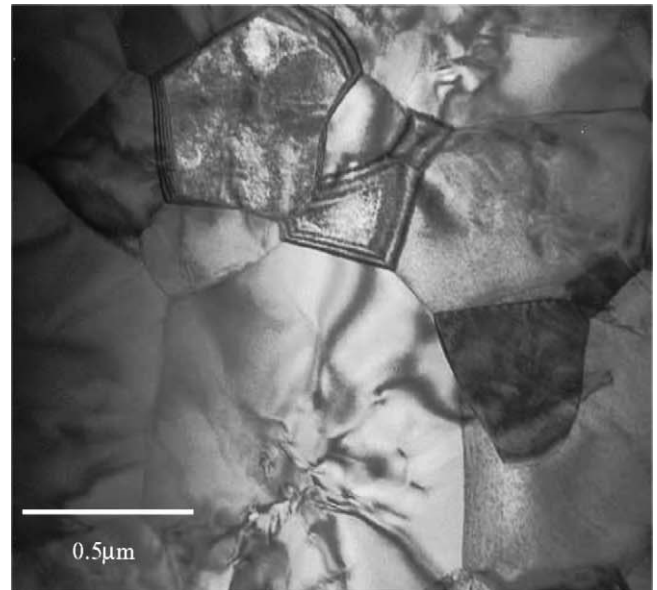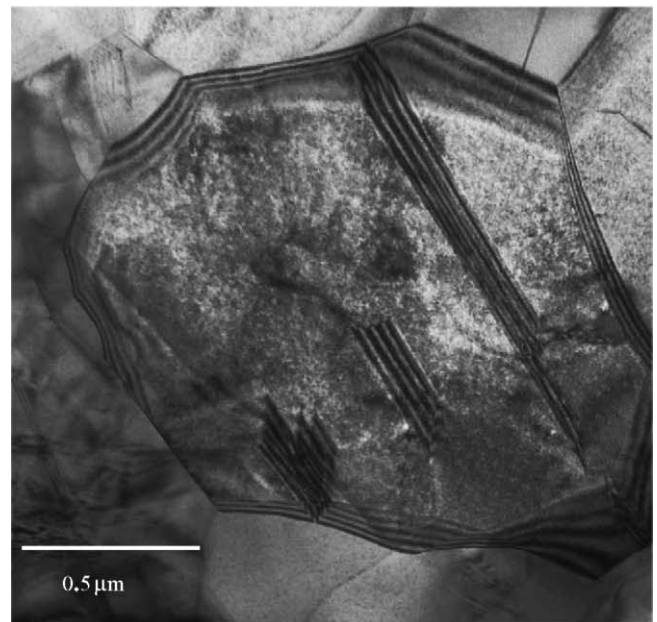
(a)

(b)

Fig. 4. TEM micrographs of sample X3 sintered for 12 h: (a) needle shaped grain (arrowed) is $Ba_8Co_1Nb_6O_{24}$; (b) grain identified by arrow is the Co-free phase $Ba_5Nb_4O_{15}$.

(a)

(b)

Fig. 5. TEM micrographs of sample X0 cooled at 60 °C/h after sintering, showing dislocations (a and b) and stacking faults (b).

This explains why the intensity of the X-ray diffraction peaks for the second phases and the volume of the secondary phases increased as non-stoichiometry increased. It is concluded that cobalt evaporation from the BCN samples was minimal in comparison with that for Zn in BZN.

Fig. 5 shows TEM images for X0 ceramics cooled at 60 °C/h after sintering. The grain size varies between 0.3 and 3 μm. The presence of dislocations can be seen throughout the microstructure. In some grains, the dislocations form a core-shell type structures in BCN. Such core-shell structures were not observed in BZN or BCZN ceramics but are common in BMN and BMT ceramics.[22] There are clear differences between the behaviour of these 1:2 ordered perovskites; subtle microstructural changes can have a significant impact on dielectric losses. Stacking faults were also frequently observed in the BCN ceramics; an example is presented in Fig. 5b for the end member $Ba(Co_{1/3}Nb_{2/3})O_3$.

In additions to dislocations and stacking faults, other sub-grain features were observed in BCN ceramics (Fig. 6). An electron diffraction pattern collected from area a in Fig. 6a along the [1 1 0] direction of the pseudocubic perovskite sub-cell is shown in Fig. 6b. The strong superlattice reflections visible at positions of $(h \pm 1/3, k \pm 1/3, l \pm 1/3)$ from the fundamental reflections originate from the Co and Nb ordering and correspond to the tripling of the cell along one unique $\langle 1\,1\,1 \rangle$ direction. The electron diffraction pattern from the area b was similar to that from area a, but the ordering was in another unique $\langle 1\,1\,1 \rangle$ direction (Fig. 6c). Thus the boundary between area a and area b is a twin, related to the anti-phase domain boundary. The FEG HRTEM image (Fig. 7a) of the two areas (shown in Fig. 6a)
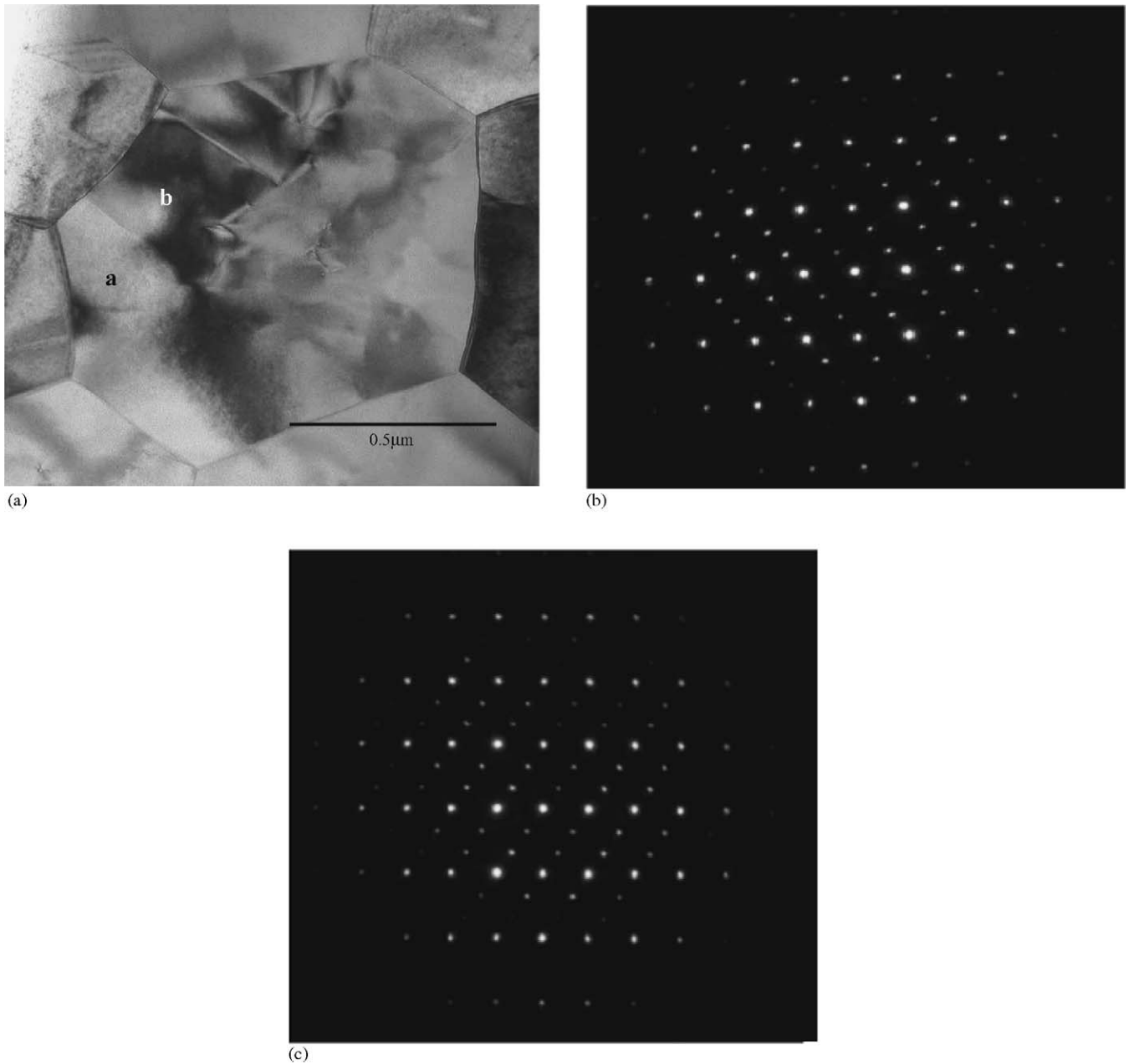
Fig. 6. TEM micrograph (a) and electron diffraction patterns (b and c) collected from areas *a* and *b* in (a), for sample X0. The electron diffraction patterns indicate that locations *a* and *b* are separated by a twin boundary.

confirms the twin relationship. Within these two areas another two types of anti-phase boundaries with displacement vectors of $\frac{1}{2}(1\,1\,0)$ and $\frac{1}{2}(1\,0\,0)$ were observed. Fig. 7b is a FEG HRTEM image showing that domain A and domain B are related by a shift of $\frac{1}{2}(1\,1\,0)$ of the cubic unit cell. Fig. 7c is a FEG HRTEM image showing that domain C and domain D are related by a shift of $\frac{1}{2}(1\,0\,0)$ of the cubic unit cell. The existence of these three types of antiphase domain boundaries has been reported for $Ba_3Co_{0.7}Zn_{0.3}Nb_2O_9$ (BCZN) ceramics.[18]

Relative permittivities and the temperature coefficient of resonant frequency for the $Ba(Co_{1/3-x}Nb_{2/3})O_3$ ceramics were almost independent of composition and processing conditions. The typical values for ε_r and τ_f were 32.4 and -14 ppm/°C,

respectively. In contrast the $Q \times f$ values were found to be sensitive to non-stoichiometry and processing conditions. Fig. 8a shows the $Q \times f$ values of BCN ceramics (sintered at 1450 °C for 4 h and cooled at 60 °C/h) as a function of composition. Stoichiometric BCN has the highest $Q \times f$ value of 38000 GHz. With increasing non-stoichiometry the $Q \times f$ values decreased to ∼34,000 GHz (X2), to 30,000 GHz (X3) to ∼15,000 GHz for sample X4. Hence stoichiometry is critically important in BCN ceramics. Even small levels of vacancies on the B sub-lattice are detrimental to the dielectric Q values.

Increasing the sintering time from 4 to 12 h caused a slight reduction in the $Q \times f$ values, typically by no more than 5%, but the losses were significantly affected by the cooling rate after
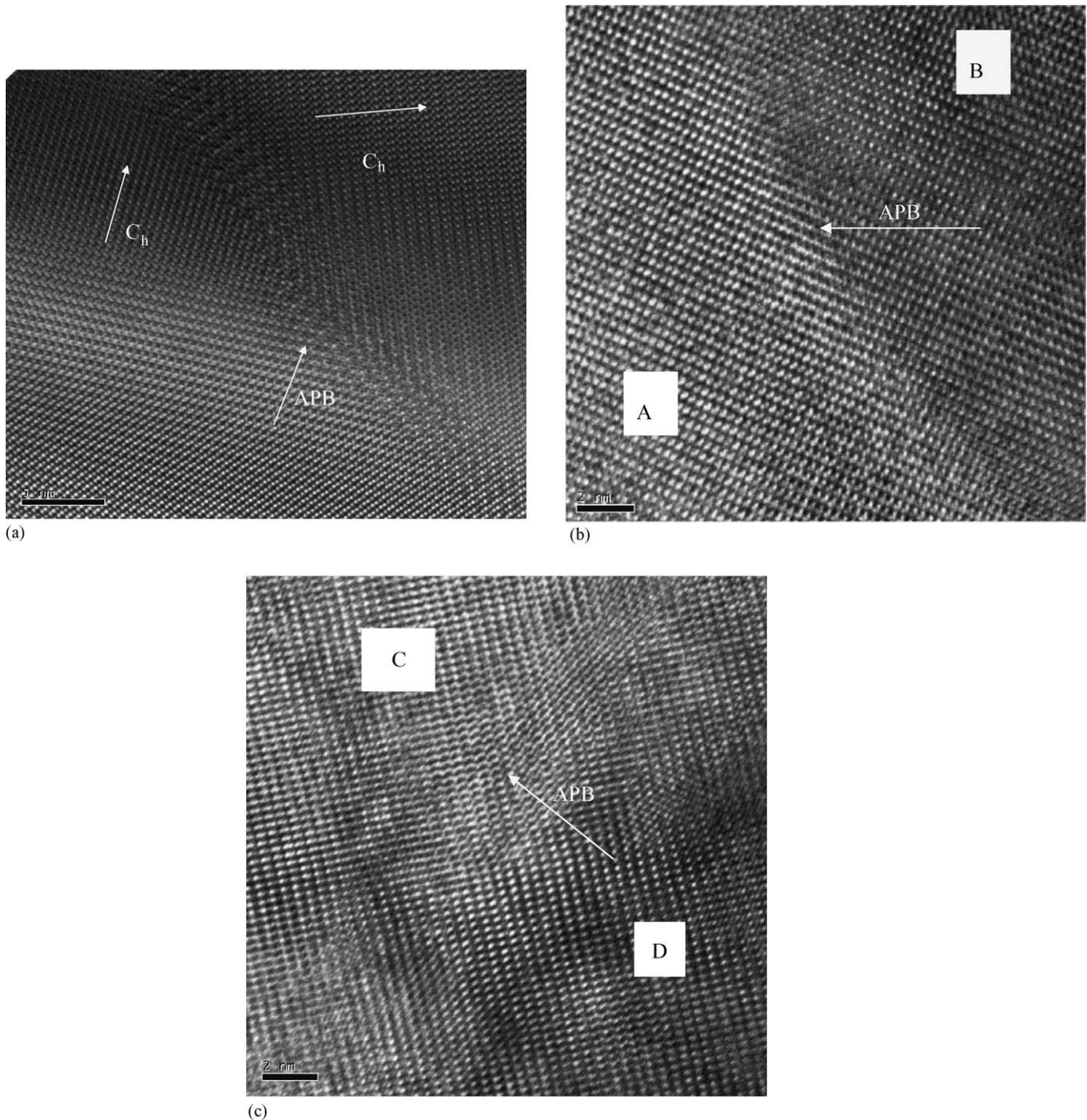
Fig. 7. FEG TEM images for sample X0. (a) Locations a and b are those shown in Fig. 6a, confirming that they are related by a twin boundary. Part (b) shows that domain A and domain B are related by a shift of $\frac{1}{2}(1\,1\,0)$ of the cubic unit cell. Part (c) shows that domain C and domain D are related by a shift of $\frac{1}{2}(1\,0\,0)$ of the cubic unit cell.

sintering (Fig. 8b). Rapidly cooled A0 samples (i.e. $360\,^{\circ}$C/h) exhibited very low $Q \times f$ values of 22,000 GHz. Reducing the cooling rate increased the $Q \times f$ values for all compositions. Sample X0 exhibited the highest $Q \times f$ values of 64,500 GHz when cooled at $5\,^{\circ}$C/h. The increase in the $Q \times f$ values on reducing the cooling rate is due to an increase in 1:2 ordering of Co and Nb cations in the hexagonal structure.

Previous studies of the effect of non-stoichiometry in complex perovskites yielded conflicting trends. Paik et al.[14] suggested Mg-deficiency (B-site) in $Ba(Mg_{1/3-x}Nb_{2/3})O_3$ was advantageous to dielectric properties. Lu and Tsai[15] reported the beneficial effects of Ba deficiency (A-site) in $Ba(Mg_{1/3}Ta_{2/3})O_3$, whilst Lee et al.[16] found that $Q \times f$ values were reduced in Mg deficient BMT (B-site modification). The present study again found B-site non-stoichiometry disadvantageous; the introduction of vacancies on the B-site must impact on the degree of ordering and affect loss mechanisms. The use of V_2O_5 as sintering aid has both advantages and disadvantages. Without it,
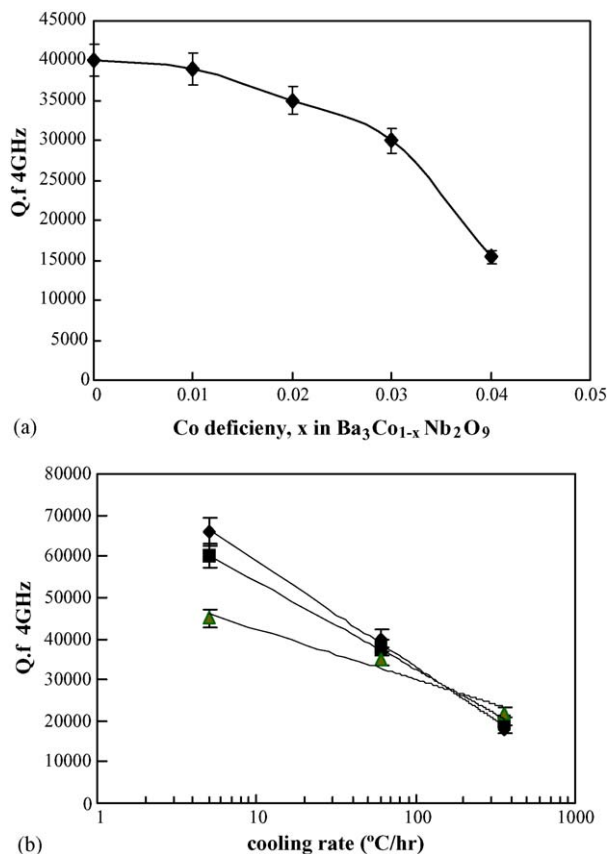
Fig. 8. Dielectric $Q \times f$ values at 4 GHz for BCN ceramics (sintered at 1450 °C for 4 h and cooled at 60 °C/h) (a) as a function of composition, (b) as a function of cooling rate after sintering (X0 (♦); X1 (■); X2 (▲)).

the samples do not achieve sufficiently high density, but there remains the question as to whether its presence degrades the $Q \times f$ values. Huang et al.[21] noted that the use of V_2O_5 as a sintering aid BMT lowered the $Q \times f$ values. Incorporation of V onto any site other than that occupied by either Nb in BCN, or Ta in BMT is likely to lead to unwanted vacancies and a reduction in the $Q \times f$ value.

4. Conclusions

High-density BCN ceramics, with a high degree of 1:2 cation ordering, were prepared with the aid of additions of vanadium oxide. Surface phases were not formed in any specimens, but cobalt deficient phases ($Ba_8Co_1Nb_6O_{24}$ and $Ba_5Nb_4O_{15}$) developed internally as non-stoichiometry increased. Three types of domain boundaries were observed in the microstructure: (i) boundaries with displacement vector of $\frac{1}{2}(1\,1\,0)$ of the cubic unit cell, (ii) boundaries with displacement vector of $\frac{1}{2}(1\,0\,0)$ of the cubic unit cell, and (iii) boundaries with twin relationships.

The microwave dielectric properties were very sensitive to the composition. The highest Q values were associated with ordered structures. Slowly cooled stoichiometric BCN ceramics exhibited $\varepsilon_r = 32$, $\tau_f \sim -10$ ppm/°C and $(Q \times f) = 66500$ at 4 GHz.

References

1. Matsumoto, H., Tamura, H. and Wakino, K., Ba(Mg,Ta)O$_3$–BaSnO$_3$ high-Q dielectric resonator. *Jpn. J. Appl. Phys.*, 1991, **30**(9B), 2347–2349.
2. Reaney, I. M., Wise, P. L., Qazi, I., Miller, C. A., Price, T. J., Cannell, D. S. *et al.*, Ordering and quality factor in 0.95BaZn$_{1/3}$Ta$_{2/3}$O$_3$–0.05SrGa$_{1/2}$Ta$_{1/2}$O$_3$ production resonators. *J. Eur. Ceram. Soc.*, 2003, **23**, 3021–3034.
3. Fukui, T., Sakurai, C. and Okuyama, M., Preparation of Ba(Mg$_{1/3}$Nb$_{2/3}$)O$_3$ ceramics as microwave dielectrics through alkoxide–hydroxide route. *J. Mater. Res.*, 1992, **7**(7), 1883–1887.
4. Azough, F., Leach, C. and Freer, R., Effect of cation order microwave dielectric properties of Ba(Zn$_{1/3}$Nb$_{2/3}$)O$_3$ ceramics. *Key Eng. Mater.*, 2002, **264–268**, 1153–1156.
5. Endo, K., Fujimoto, K. and Murakawa, K., Dielectric properties of ceramics in Ba(Co$_{1/3}$Nb$_{2/3}$)O$_3$–Ba(Zn$_{1/3}$Nb$_{2/3}$)O$_3$ solid solutions. *J. Am. Ceram. Soc.*, 1987, **70**(9), C-215–C-218.
6. Ahn, C.-W., Jang, H.-J., Nahm, S., Park, H.-M. and Lee, H.-J., Effect of microstructure on the microwave dielectric properties of Ba(Co$_{1/3}$Nb$_{2/3}$)O$_3$ and $(1 - x)$Ba(Co$_{1/3}$Nb$_{2/3}$)O$_3$–xBa(Zn$_{1/3}$Nb$_{2/3}$)O$_3$ solid solutions. *J. Eur. Ceram. Soc.*, 2003, **23**, 2473–2478.
7. Azough, F., Leach, C. and Freer, R., Effect of V$_2$O$_5$ on the sintering behaviour, cation order and properties of Ba$_3$Co$_{0.7}$Zn$_{0.3}$Nb$_2$O$_9$ ceramics. *J. Eur. Ceram. Soc.*, 2005, **25**, 2839–2841.
8. Hughes, H., Iddles, D. M. and Reaney, I. M., Niobate-based microwave dielectrics suitable for third generation mobile phone base stations. *Appl. Phys. Lett.*, 2001, **79**(18), 2952–2961.
9. Davis, P. K., Tong, J. and Negas, T., Effect of ordering-induced domain boundaries on low-loss Ba(Zn$_{1/3}$Nb$_{2/3}$)O$_3$–BaZrO$_3$ perovskite microwave dielectrics. *J. Am. Ceram. Soc.*, 1997, **80**(7), 1724–1740.
10. Kim, I. T., Kim, Y. H. and Chung, S. J., Order–disorder transition and microwave dielectric properties of Ba(Ni$_{1/3}$Nb$_{2/3}$)O$_3$ ceramics. *Jpn. J. Appl. Phys.*, 1995, **34**(Part 1, No. 8A), 4096–4103.
11. Desu, S. and O'Bryan, H. M., Microwave loss quality of Ba(Zn$_{1/3}$Nb$_{2/3}$)O$_3$. *J. Am. Ceram. Soc.*, 1985, **68**(10), 546–551.
12. Kawashima, S., Influence of ZnO evaporation on the sinterability of Ba(Zn$_{1/3}$Ta$_{2/3}$)O$_3$ ceramics. *J. Am. Ceram. Soc. Bull.*, 1993, **72**, 120–126.
13. Kim, J. S., Kim, J.-W., Cheon, C. I., Kim, Y.-S., Nahm, S. and Byun, J. D., Effect of chemical element doping and sintering atmosphere on the microwave dielectric properties of barium zinc tantalates. *J. Eur. Ceram. Soc.*, 2001, **21**, 2599–2604.
14. Paik, J. H., Kim, I. T., Byun, J. D., Kim, H. M. and Lee, J., The effect of Mg deficiency on the microwave dielectric properties of Ba(Mg$_{1/3}$Nb$_{2/3}$)O$_3$. *J. Mater. Sci. Lett.*, 1998, **17**, 1777–1780.
15. Lu, C. H. and Tsai, C. C., Reaction kinetics, sintering characteristics and ordering behaviour of microwave dielectrics barium magnesium tantalate. *J. Mater. Res.*, 1996, **5**, 1219–1227.
16. Lee, J. A., Kim, J. J., Lee, H. Y., Kim, T. H. and Choy, T. G., Effect of MgO content on microstructure evolution and microwave dielectric properties Ba(Mg$_{1/3}$Ta$_{2/3}$)O$_3$ ceramics. *Korean J. Ceram. Soc.*, 1994, **31**, 1299–1306.
17. Hughes, H., Azough, F., Freer, R. and Iddles, D., Development of surface phases in Ba(Zn$_{1/3}$Nb$_{2/3}$)O$_3$–Ba(Ga$_{1/2}$Ta$_{1/2}$)O$_3$ microwave dielectric ceramics. *J. Eur. Ceram. Soc.*, 2005, **25**, 2755–2758.
18. Azough, F., Leach, C. and Freer, R., Effect of CeO$_2$ on the sintering behaviour, cation order and properties of Ba$_3$Co$_{0.7}$Zn$_{0.3}$Nb$_2$O$_9$ ceramics. *J. Eur. Ceram. Soc*, 2006, **26**, 1883–1887.

19. Hakki, B. W. and Coleman, P. D., A dielectric resonator method of measuring inductive capacitance in the millimetre range. *IEEE Trans. Mirowave Theory Thec.*, 1980, **MTT-18**, 402–410.

20. Alchangyan, S. V. and Kislyakov, I. P., The system BaV_2O_6–$BaNb_2O_6$. *Izv. Vyssh. Uchebn. Zaved., Khim. Khim. Tekhnol.*, 1975, **18**(5), 696–698.

21. Huang, C. L., Chiang, K. H. and Chuang, S. C., Influence of V_2O_5 additions to $Ba(Mg_{1/3}Ta_{2/3})O_3$ ceramics on sintering behaviour and microwave dielectric properties. *Mater. Res. Bull.*, 2004, **39**, 629–636.

22. Barber, D. J., Moulding, K. M., Zhou, J. I. and Maoqiang, L., Structural order in $Ba(Zn_{1/3}Ta_{2/3})O_3$, $Ba(Zn_{1/3}Nb_{2/3})O_3$ and $Ba(Mg_{1/3}Ta_{2/3})O_3$ microwave dielectric ceramics. *J. Mater. Sci.*, 1997, **32**, 1531–1544.